

Patch End-Launchers—A Family of Compact Colinear Coaxial-to-Rectangular Waveguide Transitions

Massimiliano Simeoni, *Member, IEEE*, Cristian I. Coman, *Member, IEEE*, and Ioan E. Lager, *Member, IEEE*

Abstract—A new family of structures launching the fundamental mode in rectangular waveguides is proposed. Individual or stacked cavity-backed patch antennas radiate into a rectangular waveguide, providing a good matching with a coaxial input over a wide frequency range. The configuration results in a very compact, colinear transition from a standard coaxial connector to a rectangular waveguide. The components have applications as general-purpose coaxial-to-rectangular waveguide transitions and are well suited for low-profile, phased-array antennas. Experimental results confirm the computational estimations of the proposed components' performance.

Index Terms—Coaxial waveguides, electromagnetic launching, waveguide junctions, waveguide transitions.

I. INTRODUCTION

COLINEAR end-launcher coaxial-to-rectangular waveguide transitions are found to be convenient in many applications, in particular for feeding phased-array antennas consisting of closely packed radiators. In such cases, the use of the standard, right-angle coaxial-to-rectangular waveguide transitions is highly inadequate, the traditional solution being that of employing coaxial, L-shaped loop launchers [1]–[4].

An alternative to the L-shaped loop launchers has been proposed in [5]. The configuration consisted of a cavity-backed patch antenna [6], [7] that radiates into a rectangular waveguide, in view of exciting the fundamental (TE₋) mode. The patch is fed from the back by means of a coaxial cable whose internal conductor protrudes through the substrate on which the patch is located. The length of the launcher (hereafter referred to as the *patch end-launcher*) is essentially determined by the substrate's thickness, with the resulting transition being, thus, extremely short. The proposed configuration provides an excellent matching of the coaxial input to the rectangular waveguide at a single frequency, complemented by an acceptable matching over a relatively wide frequency. For example, the *X*-band patch end-launcher demonstrated in [5] was characterized by an input reflection coefficient lower than -10 dB over a fractional bandwidth of up to 14%. Furthermore, that patch end-launcher was compared with an L-shaped loop-launcher tuned at the same fre-

quency, resulting in both an enlargement of the operational frequency band and in a substantial reduction of the transition's length.

The concept introduced in [5] is now generalized by proposing *multituned, patch end-launchers*. Stacked patch antennas that radiate into rectangular waveguides are employed for exciting the fundamental mode. The use of multituned structures yields optimum matching at more frequencies and allows a significant widening of the operational frequency band of the coaxial-to-rectangular waveguide transition (fractional bandwidths ranging up to 25% in the *X*-band being easily achieved by means of a doubly tuned patch end-launcher).

The paper now proceeds by briefly revisiting the patch end-launcher. The doubly tuned patch end-launcher is then described in detail in Section III. Some results of computer simulations concerning singly and doubly tuned end-launchers designed for operating in the *X*-band are presented in Section IV. These preliminary studies are supplemented in Section V by a sensitivity analysis, examining the influence of small dimensional deviations on the launchers' performance. The experimental validation of these numerical results is discussed in Section VI, where details referring to the manufacturing process of the end-launchers and the adopted measurement setup will be provided as well. The paper is concluded with a general discussion (included in Section VII) and by drawing some conclusions.

II. SINGLY TUNED PATCH END-LAUNCHER

The singly tuned patch end-launcher (which is depicted in Fig. 1) consists of a circular metallic patch that is etched on a plated microstrip laminate. The device can be interpreted as a cavity-backed patch antenna that radiates into a rectangular waveguide or as a cascade of guiding structures. The latter approach permits a description of the junction's functioning in terms of modal couplings between the modes of the different guiding structures composing the end-launcher (see [5]).

The device at the core of this work ensures the matching between the coaxial line input and the rectangular waveguide output. Since the matching is optimum at a single frequency (hereafter referred to as f_m), we denote it as a *singly tuned patch end-launcher*. Note that the frequency where the best matching is achieved depends, essentially, on the patch's radius r_p and on the substrate's permittivity and thickness h_d (see Fig. 1).

III. DOUBLY TUNED PATCH END-LAUNCHER

As already anticipated in [5], the concept at the basis of the patch end-launcher can be extended to multiply tuned configura-

Manuscript received August 29, 2005; revised December 8, 2005.

The authors are with the Faculty of Electrical Engineering, International Research Centre for Telecommunications-Transmission and Radar, Mathematics and Computer Science, Delft University of Technology, 2628 CD Delft, The Netherlands (e-mail: m.simeoni@ircr.tudelft.nl).

Digital Object Identifier 10.1109/TMTT.2006.871923

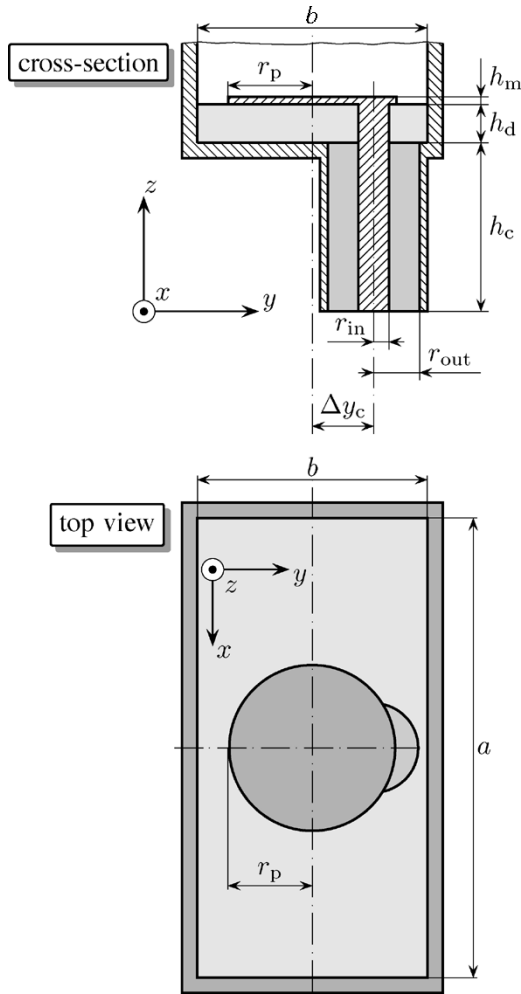


Fig. 1. Singly tuned patch end-launcher.

tions by employing a strategy that is reminiscent of the approach used for designing the doubly tuned loop launcher described in [4]. Basically, it amounts to optimizing the matching between the structure's input and output ports at a number of relatively closely spaced frequencies such that to broaden the frequency band of operation.

A straightforward solution to obtaining a multiply tuned structure is by stacking several patches on top of each other. In particular, a doubly tuned patch end-launcher is obtained by stacking two metallic patches; this solution has a long history of application in the realm of radiating elements [8], [9]. The proposed geometry (see Fig. 2) consists of two stacked patches located on dielectric substrates, where the lower one is fed by means of a coaxial line whose inner conductor protrudes through the lowermost substrate. No metallic connection between the two patches is required, as the proximity ensures their electromagnetic coupling [10]. When also considering the metallic enclosure consisting from the waveguide's walls and the ground plane, the overall structure is analogous to a cavity-backed, stacked patch antenna [6], [7].

By properly choosing the radii of the patches and their relative spacing, two resonances can be found and tuned to desired values. The two resonance frequencies are denoted in the following as f_l and f_h . For the case when the spectral spacing

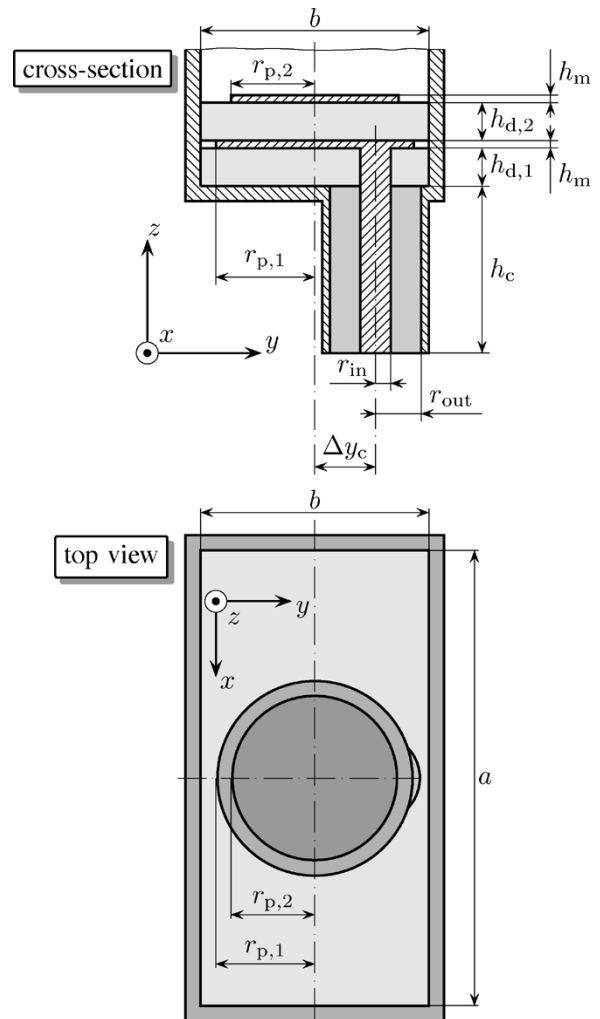


Fig. 2. Doubly tuned patch end-launcher.

between the two resonances is large, the device operates in two separate frequency bands that separated by an intermediate stop-band. Nevertheless, when the two resonances are close in the spectral domain, they generate a region of "constructive interference" in the enclosed frequency range. A good level of transmission between the access ports can then be obtained in that frequency region, resulting in a substantial increase of the device's operational bandwidth. Furthermore, the level of matching between the input and the output ports can be controlled by adjusting the location of the feeding point and the spacing between the two patches, together with adequately choosing the permittivity of the dielectric substrates. The description of the device's functioning mechanism is concluded by once again stressing the fact that the proposed configuration can be assimilated to a cascade of guiding structures. Consequently, its behavior can be investigated by employing the instruments of the modal analysis of planar waveguide junctions [5], [11]–[13].

IV. X-BAND END-LAUNCHERS

The performance of the components presented in Sections II and III is illustrated by examining two end-launchers that are intended to operate in the X-band. Both launchers are designed and optimized by using the commercial software package CST

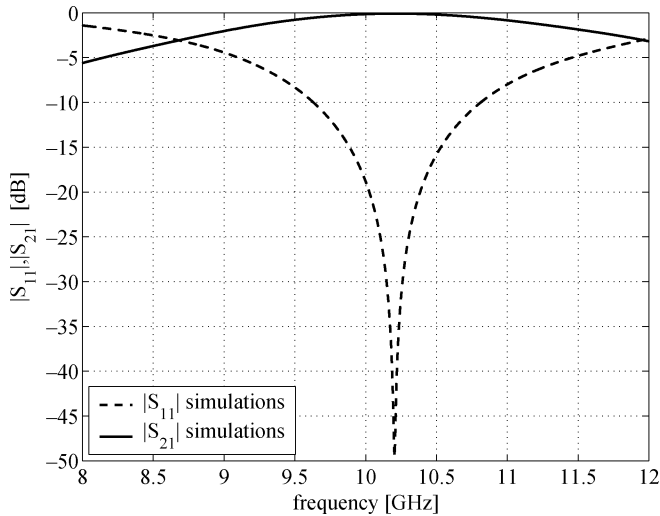


Fig. 3. Simulated frequency response of the singly tuned end-launcher.

Microwave Studio, version 5.0 [14]. Note that the analysis of the singly tuned end-launcher has already been described in detail in [5]. Nevertheless, the relevant results are reiterated to provide the basis of the comparison with the physical measurements reported in Section VI.

Both launchers use the same input and output ports. A standard subminiature A (SMA) coaxial connector (having the characteristic dimensions $r_{in} = 0.65$ mm, $r_{out} = 2.05$ mm and the insulator's relative permittivity $\epsilon_{r,c} = 2.08$) is adopted as input port. The output port is a standard WR 90 rectangular waveguide, with $a = 22.86$ mm and $b = 10.16$ mm (see Figs. 1 and 2). In view of its favorable electric properties, availability and ease of processing by means of standard lithographic etching technology, a Rogers RO4003C (Hydrocarbon ceramic) microstrip laminate is selected as material for manufacturing the end-launchers. Consequently, based on the product specifications (see [15]), the substrate's relative permittivity amounts to $\epsilon_{r,d} = 3.38$, its dissipation factor to $\tan \delta = 0.0027$ (at 10 GHz), and the thickness of the patches equals that of the metallization layer, i.e., $h_m = 35$ μm (see Figs. 1 and 2). A conductivity of $\sigma = 5.8 \times 10^7$ S/m (copper) is assumed for all of the metallic parts.

A. Singly Tuned X-Band End-Launcher

Following the procedure described in [5], the launcher is designed for optimum matching at 10.2 GHz. The patch's radius r_p is taken as 4.00 mm and the substrate's thickness h_d amounts to 1.524 mm. For optimally tuning the component, the coaxial connector is shifted away from the patch's center by $\Delta y_c = 2.0$ mm (see Fig. 1). Hereafter, the coaxial connector and the rectangular waveguide are denoted as the ports 1 and 2, respectively.

The simulated frequency response of the component is displayed in Fig. 3. The component is optimally matched at a frequency of 10.2 GHz and exhibits an input reflection coefficient $|S_{11}|$ lower than -10 dB over a fractional bandwidth of roughly 10%. An insertion loss $|S_{21}|$ of about 0.05 dB is observed at the frequency of best matching.

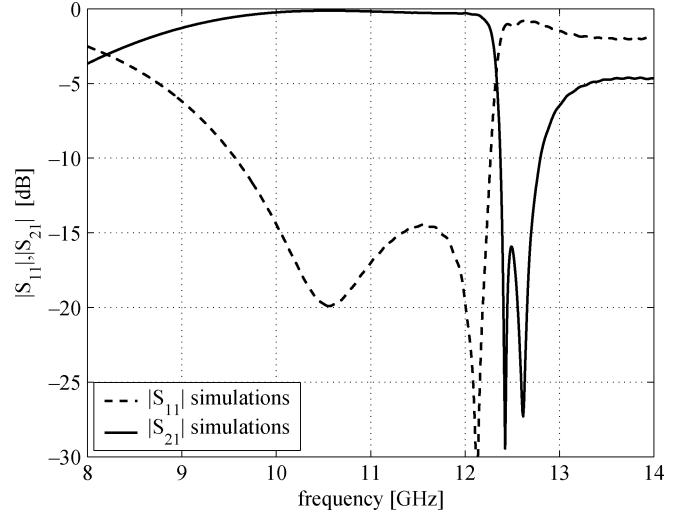


Fig. 4. Simulated frequency response of the doubly tuned end-launcher.

B. Doubly Tuned X-Band End-Launcher

The design of a doubly tuned patch end-launcher requires the definition of a number of parameters such as: the patches' radii $r_{p,1}$ and $r_{p,2}$, the spacing between the patches $h_{d,2}$, the dielectric permittivity and the thicknesses of the dielectric substrates $h_{d,1}$ and $h_{d,2}$, and the shift of the coaxial connector Δy_c (see Fig. 2).

The choice for the substrates' permittivity and thicknesses is clearly limited by the availability of the microstrip laminates. In the present case, it was decided to use the same kind of laminates for both substrates, namely, Rogers RO4003C. Consequently, the substrate's relative permittivity was $\epsilon_{r,d} = 3.38$ and its dissipation factor $\tan \delta = 0.0027$ (at 10 GHz), while the thicknesses of the substrates were chosen from the catalog data as $h_{d,1} = 1.524$ mm and $h_{d,2} = 0.508$ mm, respectively. Furthermore, numerical simulations demonstrated that choosing two patches having identical radii $r_{p,1} = r_{p,2} = 3.65$ mm results in an optimum performance of the launcher. Finally, a parameter study has yielded an optimum off axis shift of the coaxial connector of $\Delta y_c = 2.8$ mm (see Fig. 2).

The computed frequency dependence of the input reflection and transmission coefficients ($|S_{11}|$ and $|S_{21}|$, respectively) is depicted in Fig. 4 (where the ports are denoted as in the case of the singly tuned end-launcher). The former parameter is lower than -10 dB over the frequency band ranging from 9.6 to 12.3 GHz, yielding an operational relative bandwidth of approximately 24%. At the same time, $|S_{11}|$ is lower than -14 dB over the frequency band ranging from 10 to 12.2 GHz (which translates into a relative bandwidth of about 20%). The in-band insertion-loss level is approximately 0.1–0.2 dB.

V. SENSITIVITY ANALYSIS

The devices described by this contribution are meant to be mass-produced. It is then extremely important to have a clear understanding of the effect of small dimensional deviations on the launchers' performance. In this respect, it is first observed that the parameters of the microwave laminates (i.e., the thicknesses of the dielectric and of the metal plating and the permittivity) can be assumed to be virtually exact. It then follows that

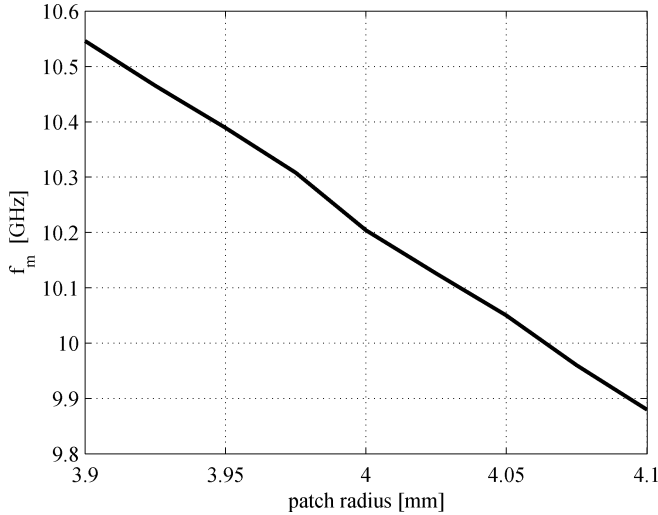


Fig. 5. Dependence of f_m on small variations of r_p .

the only parameters that are subject to (technological) inaccuracies are the dimensions and the location of the patches and the off axis shift of the feeding points. Since the resonant frequency *mainly* depends on the patches' radii, a sensitivity analysis was conducted in order to estimate the frequency shift due to (possible) manufacturing limitations.

The examination of the effect of small dimensional deviations was conducted by means of numerical experiments. The limits of the relevant studies were chosen in accordance to the dimensional precision indicated by the producer of the printed boards, i.e., $\pm 100 \mu\text{m}$.

In the case of the singly tuned end-launcher, the sensitivity analysis has predicted variations of the resonant frequency within the range of 600 MHz; the complete dependence is shown in Fig. 5.

A similar study was conducted for the doubly tuned launcher as well. Nevertheless, in this case, the effect of small perturbations simultaneously affecting *two* parameters, namely, the radii $r_{p,1}$ and $r_{p,2}$, must be accounted for. The dependence of f_l and f_h on the variations of $r_{p,1}$ and $r_{p,2}$ is displayed in Figs. 6 and 7, respectively. From them, it can be observed that the frequency excursions amounted to 800 and 500 MHz in the case of the f_l and f_h frequencies, respectively.

The numerical experiments clearly indicate the necessity to ensure a very high accuracy of the dimensions of the patches. In any case, the $\pm 100 \mu\text{m}$ accuracy guaranteed by the manufacturer of our prototypes seems insufficient for obtaining precision end-launchers. In fact, this aspect became evident during the measurement of the manufactured launchers, which will be discussed in Section VI-B.

VI. EXPERIMENTAL VALIDATION

For validating the computational estimations of the performance of the proposed devices, a number of singly and doubly tuned end-launchers was fabricated and measured. The results of the physical measurements are hereafter presented.

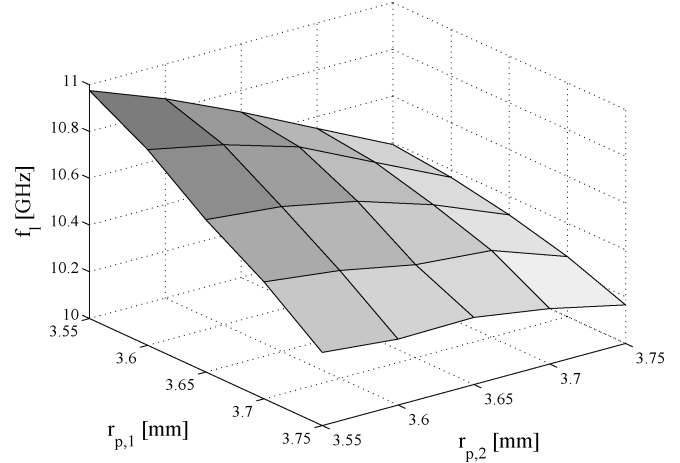


Fig. 6. Dependence of f_l on small variations of $r_{p,1}$ and $r_{p,2}$.

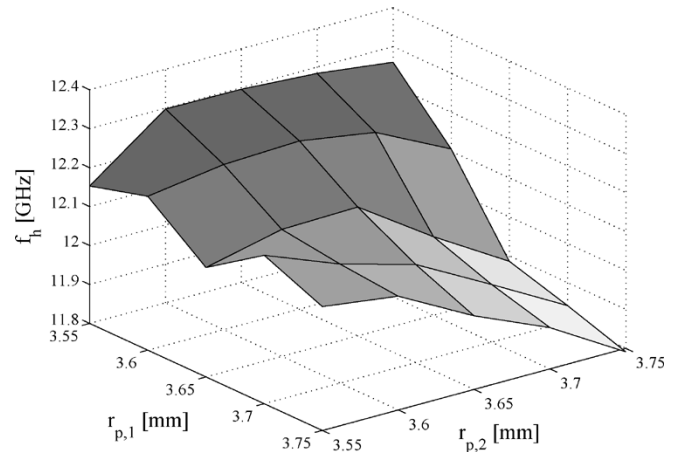


Fig. 7. Dependence of f_h on small variations of $r_{p,1}$ and $r_{p,2}$.

A. Manufacturing of the Prototypes

The prototypes of the singly and doubly tuned end-launchers were manufactured in printed technology. Both of the dielectric boards and the pertaining flanges employed for mounting the launcher on the waveguide ends have been obtained from commercially available microstrip boards. The components needed to assemble the singly and the doubly tuned launchers are depicted in Figs. 8 and 9, respectively. A metal-plated hole is employed for allowing the protruding pin to pass through the dielectric substrate. The metal plating of the hole ensures the electrical connection between the coaxial connector's inner pin and the metallic patch. The location of the hole coincides with that of the feeding points in Figs. 1 and 2. The flanges needed for attaching the launchers to the waveguide ends are realized of dielectric boards that are metal-plated on both faces. Four fine holes are provided for aligning the flange with the dielectric substrate. Additionally, mounting holes are drilled in the flange for fastening the device to the waveguide. Finally, one large metal-plated hole is included in the design for allowing the insertion of the coaxial connector directly behind the substrate.

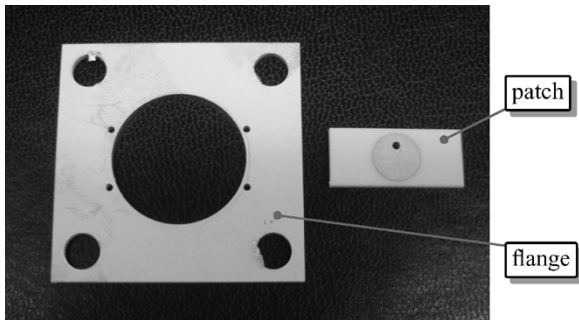


Fig. 8. Components of the singly tuned patch end-launcher.

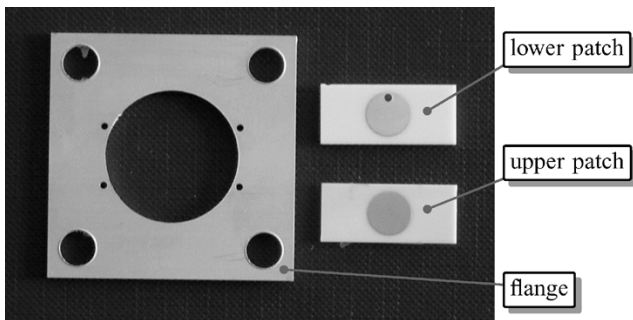


Fig. 9. Components of the doubly tuned patch end-launcher.

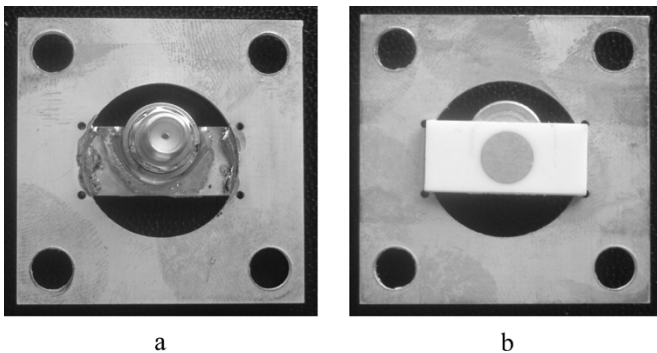
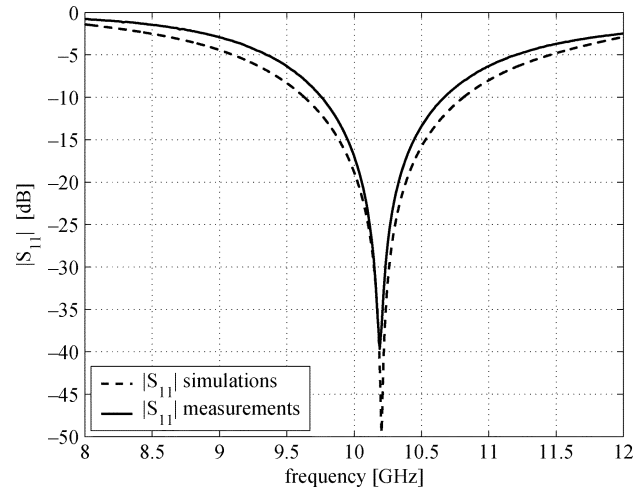
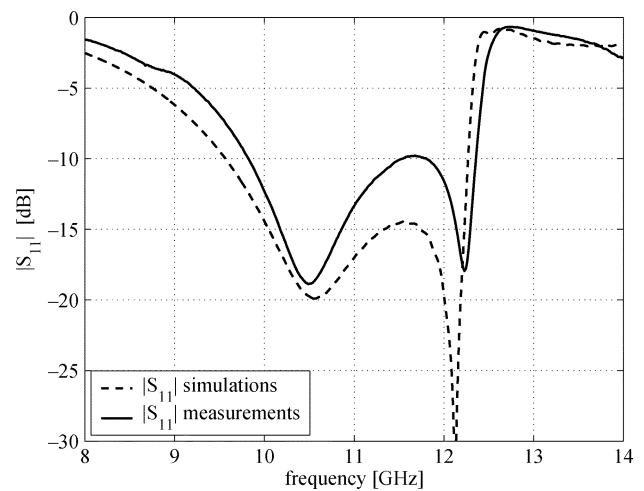


Fig. 10. Assembled doubly tuned end-launcher. (a) Back view. (b) Top view.

A three-step procedure is applied for assembling the singly tuned patch launcher. First, the inner conductor of the coaxial connector is passed through the relevant metal-plated hole and soldered to the inner surface of the hole itself. Subsequently, the ground conductor of the connector is soldered to the back side of the substrate. Finally, the substrate is aligned with respect to the flange, and its (metal-plated) back-side is soldered to the sidewalls of the large metal-plated hole of the flange. This assembling procedure ensures an electric connection between the flange, the back-side of the substrate, and the ground conductor of the coaxial connector. As for the assembling of the doubly tuned end-launcher, this requires a supplementary step. After executing the three steps indicated above, the second substrate is stacked and glued on top of the first one. The fully assembled *doubly tuned end-launcher* is shown in Fig. 10.

B. Measured Results

The manufactured prototypes have been measured with a Agilent 8722ES vectorial network analyzer. A full two-port

Fig. 11. Measured $|S_{11}|$ -parameter for the singly tuned end-launcher and comparison with the computational results.Fig. 12. Measured $|S_{11}|$ -parameter for the doubly tuned end-launcher and comparison with the computational results.

calibration has been performed by means of a coaxial waveguide calibration kit. Two different setups have been used for measuring the $|S_{11}|$ - and $|S_{21}|$ -parameters of the manufactured prototypes.

The first setup, which was used for the measurement of the $|S_{11}|$ -parameter, consists of the mounting the device under test (DUT) on the flange of a rectangular waveguide (standard WR 90) loaded with a waveguide-matched load. In this case, the reflection coefficient measured at the coaxial input of the DUT correspond to the $|S_{11}|$ -parameter of the DUT itself, since we can assume a wave of negligible magnitude being reflected backward by the matched waveguide termination. The measured $|S_{11}|$ -parameter corresponding to the singly and the doubly tuned patch end-launchers is illustrated in Figs. 11 and 12, respectively.

The second setup, which was used in the measurement of the $|S_{21}|$ -parameter, consists of mounting the DUT on the flange of a rectangular waveguide (standard WR 90) connected at the other end (port 2) to a commercial right-angle coaxial-to-rectangular waveguide transition of the type described in [16]. The transmission coefficient relative to the TEM-mode propagating

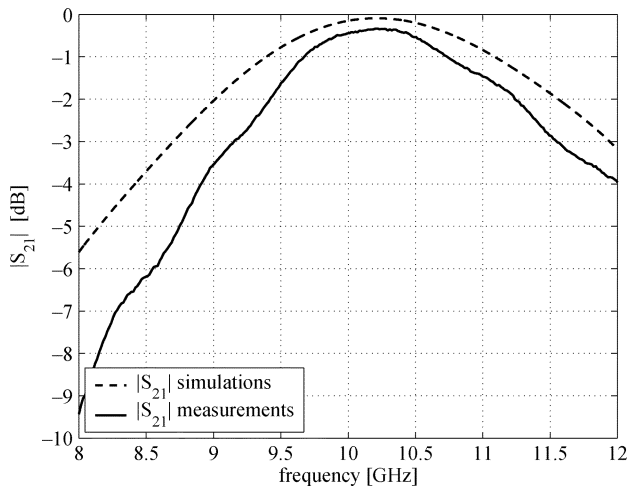


Fig. 13. Measured $|S_{21}|$ -parameter for the singly tuned end-launcher and comparison with the computational results.

through the coaxial cables was measured. The contribution to the insertion loss introduced by the right-angle transition has been separately evaluated¹ and subtracted from the measured parameter. The measured transmission coefficient can then be assimilated to the $|S_{21}|$ -parameter of the DUT even if the reference plane defining port number 2 is placed at the coaxial input of the right-angle coaxial-to-rectangular waveguide transition and not at its waveguide flange. It should be noted that, because of this different definition of the electric ports, a discrepancy between the computed and measured $|S_{21}|$ -parameters is bound to manifest itself. The measured $|S_{21}|$ -parameters corresponding to the singly and the doubly tuned patch end-launchers are illustrated in Figs. 13 and 14, respectively.

Upon returning to the $|S_{11}|$ -parameter, we can observe a good agreement between the measured and computed results related to the singly tuned end-launcher. In the case of the doubly tuned end-launcher, an excessive return loss is observed in the middle of the passband. The excessive reflection is probably due to the inaccuracies introduced during the assembly of the prototypes, in particular, for the alignment of the stacked boards. The return loss, however, remains lower than 10 dB over a frequency range of approximately 2.5 GHz.

For the $|S_{21}|$ -parameter, as anticipated, there is a small discrepancy between the computationally estimated and measured results that can be attributed to a combination of causes:

- different definitions of port 2 in the experimental phase and in the numerical simulation;
- imperfections occurring in the manufacturing of the prototypes, especially during the assembling process.

¹The contribution of the right-angle transition to the measured insertion loss has been experimentally evaluated. Two identical right-angle transitions have been connected to each other at their waveguide ends, and the transmission coefficient between the two coaxial inputs has been measured. The insertion loss measured was then divided by two to obtain the contribution of the individual transition. Note that this procedure does not represent a rigorous shift of the reference plane of port 2 from the coaxial input of the right-angle transition to its waveguide end, but merely compensates for the insertion losses introduced by the transition itself.

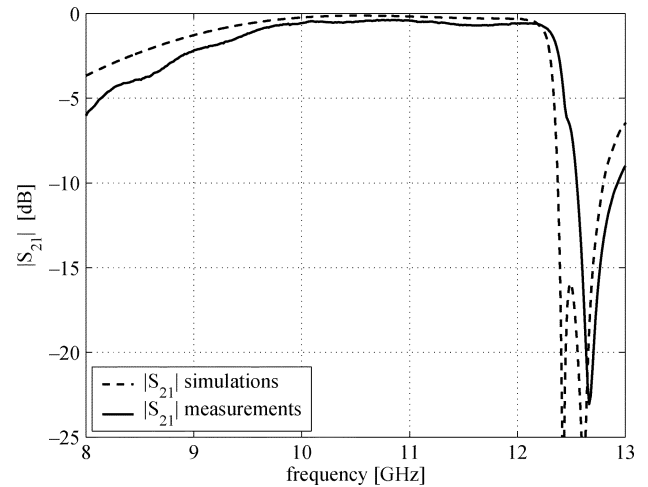


Fig. 14. Measured $|S_{21}|$ -parameter for the doubly tuned end-launcher and comparison with the computational results.

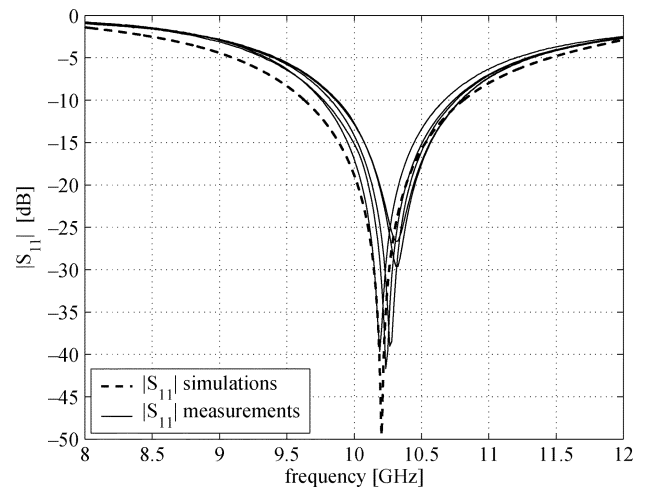
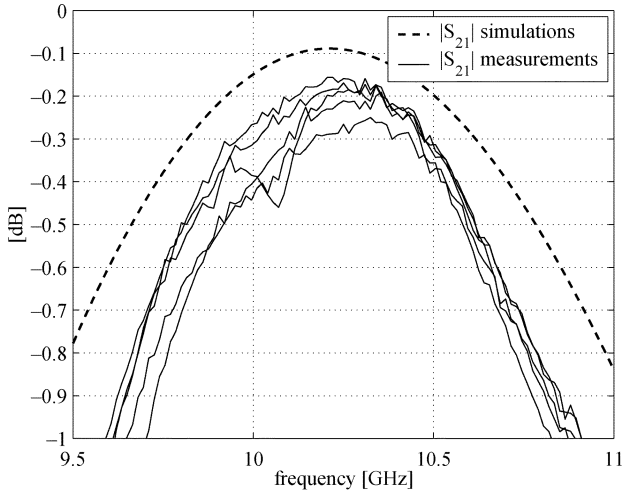


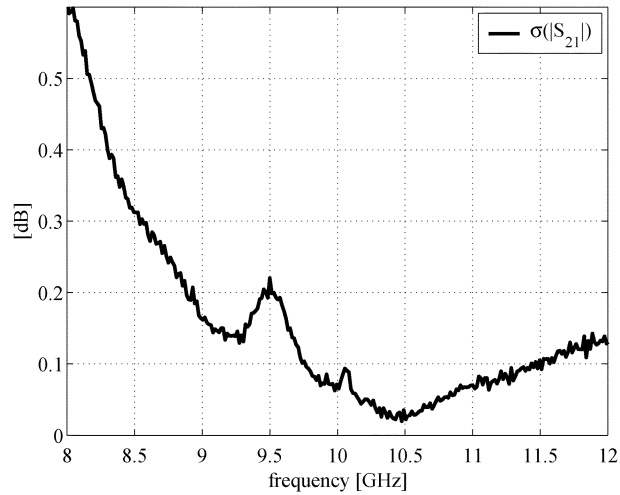
Fig. 15. Measured $|S_{11}|$ -parameter for a sample of five singly tuned end-launchers and comparison with the computational results.

As concerns the impact of the last cause, it is further substantiated by the fact that the discrepancy is more visible in the case of the doubly tuned end-launcher (see Fig. 14), the assembling of which consisted of more operations that are prone to introduce manufacturing inaccuracies. Nevertheless, an insertion loss of approximately 0.15 dB is observed at $f = f_m$ for the singly tuned patch launcher. The insertion loss remains above 0.4 dB over a frequency range of roughly 700 MHz. As for the doubly tuned patch launcher, an insertion loss of less than 1 dB is observed over a frequency band of roughly 2.5 GHz.

In order to assess the reproducibility of the designed devices, which is an aspect that is of paramount importance in the case of a mass production of such components, a sample of five end-launchers of both types were measured; the results of this analysis are reported in Figs. 15–18. The overlapping of the curves is very good, except for the region in the proximity of resonances where, as a result of small shifts in the resonant frequencies, larger spreads of the $|S_{11}|$ curves are observed. For obtaining a quantitative measure of the spread of the measured characteristics (in particular, as concerns the $|S_{21}|$), the

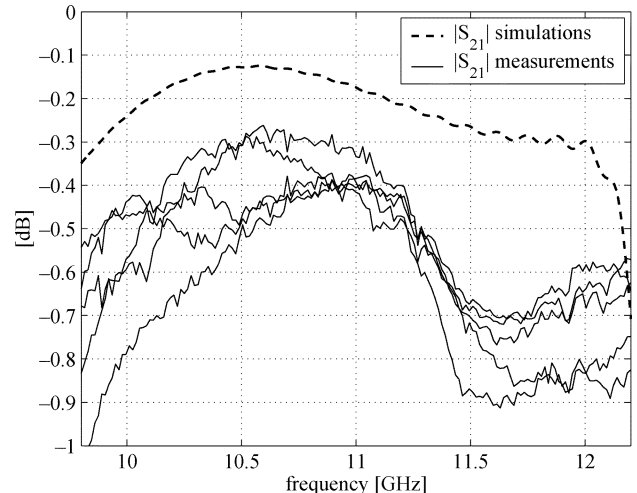


a

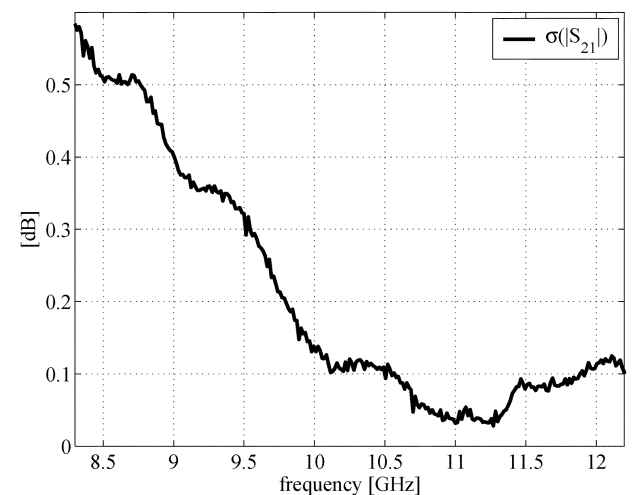


b

Fig. 16. Measured $|S_{21}|$ -parameter for a sample of five singly tuned end-launchers. (a) Measured and computational results. (b) Frequency dependence of the standard deviation σ .



a



b

Fig. 18. Measured $|S_{21}|$ -parameter for a sample of five doubly tuned end-launchers. (a) Measured and computational results. (b) Frequency dependence of the standard deviation σ .

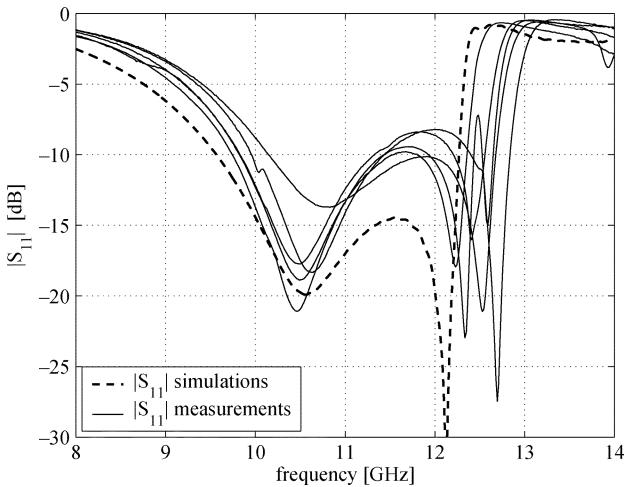


Fig. 17. Measured $|S_{11}|$ -parameter for a sample of five doubly tuned end-launchers and comparison with the computational results.

values of the standard deviation are very small (below 0.6 dB) within the frequency band of interest.

VII. DISCUSSION

As demonstrated by the measurement results reported in Section VI-B, the manufacturing technology has a determinant role in ensuring adequate performance of the components. Although the reproducibility test has pointed toward a relatively low sensitivity to (small) fabrication inaccuracies, it is obvious that, in order to guarantee the performance as estimated by the numerical simulations, the technology employed for producing such devices should be revisited. In this respect, the examined prototypes suffered from a number of manufacturing flaws, particularly in the assembling phase. The most commonly observed defect was the slight misalignment of the two substrates that compose the doubly tuned launchers. Furthermore, as the upper layer is extremely thin (0.508 mm), it tends to bend, leaving some air gap of irregular shape between the two dielectric boards. Finally, the gluing procedure is not easy to control, and the electric properties of the employed adhesive were

frequency dependence of their standard deviation σ was computed; this parameter is plotted in Figs. 16(b) and 18(b). The

unknown. All of these shortcomings can be addressed by an industrial fabrication of the components. Standard printed circuits board (PCB) technology enables the manufacturing of sealed structures composed of multiple dielectric boards, including metallic layers and vertical interconnections (via-holes). The PCB technology is then recommended for manufacturing these components.

Upon returning to the concept at the basis of the design of the patch end-launchers, it can be mentioned that a further broadening of the operational bandwidth can be achieved by moving toward larger numbers of stacked patches. Alternatively, configurations containing patches with different shapes (i.e., square and triangular) may also be considered. Nevertheless, it must be stressed that, in all cases, particular attention must be paid to ensuring the field purity of the launched wave. To substantiate this, it is noted that, irrespective of the patch's shape, undesired field components are excited as well. Depending on the magnitude of these components, their suppression requires the use of a section of monomodal waveguide, as this length is interrelated to the shape of the patch. By recalling the fact that this research focused on *compact waveguide structures*, it is obvious that an optimization of the patch's shape will always be needed.

VIII. CONCLUSION

The performance of a new family of structures launching the fundamental mode in rectangular waveguides was discussed. Singly and multiply tuned launchers consisting of (stacked) patches were proposed for matching a coaxial input to a rectangular waveguide over a frequency range as wide as possible. The examined configurations provide an extremely flat, colinear transition from a standard coaxial connector to the relevant waveguide. Computational simulations and experimental results were employed for validating the advocated concept. Numerical simulations (finite-difference time domain) show an insertion-loss level of approximately 0.1–0.2 dB in the frequency band of operation. The proposed components are amenable to fabrication in a standard PCB technology.

ACKNOWLEDGMENT

The authors would like to acknowledge the support provided by A. Allstaff (ESA-ESTEC) and Dr. M. Spirito (Delft University of Technology) during the experimental phase of this work.

REFERENCES

- [1] R. Tang and N. S. Wong, "Multimode phased array element for wide scan angle impedance matching," *Proc. IEEE*, vol. 56, no. 11, pp. 1951–1959, Nov. 1968.
- [2] M. D. Desphande, B. N. Das, and G. S. Sanyal, "Analysis of an end launcher for an X-band rectangular waveguide," *IEEE Trans. Microw. Theory Tech.*, vol. MTT-27, no. 8, pp. 731–735, Aug. 1979.
- [3] S. M. Saad, "A more accurate analysis and design of coaxial-to-rectangular waveguide end launcher," *IEEE Trans. Microw. Theory Tech.*, vol. 38, no. 2, pp. 129–134, Feb. 1990.
- [4] V. Galdi, G. Gerini, M. Guglielmi, H. J. Visser, and F. D'Agostino, "CAD of coaxially end-fed waveguide phased-array antennas," *Microw. Opt. Technol. Lett.*, vol. 34, no. 4, pp. 276–281, Aug. 20, 2002.

- [5] M. Simeoni, C. Coman, and I. E. Lager, "Compact colinear end-launcher for rectangular waveguides," in *IEEE MTT-S Int. Microw. Symp. Dig.*, Long Beach, CA, Jun. 2005, pp. 1199–1202.
- [6] G. Gentili, F. Perez-Martinez, M. Salazar-Palma, and L. Garcia-Castillo, "Analysis of single and stacked microstrip patch antennas residing in a cavity by a Green's function technique," in *Proc. IEEE AP-S Proc. Antennas Propag. Soc. Int. Symp.*, Jun. 1994, pp. 944–947.
- [7] J. Rubio, M. A. Gonzalez, and J. Zapata, "Analysis of cavity-backed microstrip antennas by a 3-D finite element/segmentation method and a matrix Lanczos–Pad algorithm (SFELP)," *IEEE Antennas Wireless Propag. Lett.*, vol. 1, pp. 193–195, 2002.
- [8] S. A. Long and M. D. Walton, "A dual-frequency stacked circular disc antenna," *IEEE Trans. Antennas Propag.*, vol. AP-27, no. 3, pp. 270–273, Mar. 1979.
- [9] A. Sabban, "A new broadband stacked two-layer microstrip antenna," in *Proc. IEEE AP-S Proc. Antennas Propag. Soc. Int. Symp.*, May 1983, pp. 63–66.
- [10] H. Oltman and D. Huebner, "Electromagnetically coupled microstrip dipoles," *IEEE Trans. Antennas Propag.*, vol. AP-29, no. 1, pp. 151–157, Jan. 1981.
- [11] M. Simeoni, D. Schmitt, V. E. Boria, and S. Marini, "Efficient full-wave CAD tool of passive components based on coaxial waveguide junctions," in *Proc. IEEE MTT-S Int. Microw. Symp. Dig.*, Fort Worth, TX, Jun. 2004, pp. 1045–1048.
- [12] M. Simeoni, "A note on the evaluation of modal coupling coefficients at planar waveguide junctions," *Int. J. Numer. Model.*, vol. 18, no. 3, pp. 221–226, May–Jun. 2005.
- [13] G. Conciauro, M. Guglielmi, and R. Sorrentino, *Advanced Modal Analysis*. New York: Wiley, 2000.
- [14] CST MICROWAVE STUDIO, *Tutorials CST-Computer Simulation Technol.* Darmstadt, Germany, 2003.
- [15] Rogers Corporation—Advanced Circuit Materials Div., *High Frequency Laminates Literature Index* [Online]. Available: <http://www.rogerscorporation.com>
- [16] M. E. Bialkowski, "Analysis of a coaxial-to-waveguide adaptor including a discent probe and a tuning post," *IEEE Trans. Microw. Theory Tech.*, vol. 43, no. 2, pp. 344–349, Feb. 1995.



Massimiliano Simeoni (S'96–M'02) was born in Rieti, Italy, on July 4, 1974. He received the Laurea degree (*summa cum laude*) from the University of Perugia, Perugia, Italy, in 1999, and the Ph.D. degree in microwave and optical communications from the University of Limoges, Limoges, France, in 2002.

From June 2002 to April 2004, he was with the European Space Research and Technology Center (ESTEC), European Space Agency (ESA), Noordwijk, The Netherlands, as Research Fellow.

In May 2004, he joined the International Research Centre for Telecommunications-Transmission and Radar, Delft University of Technology, Delft, The Netherlands. His research interests include the numerical characterization of guiding structures, waveguides discontinuities, microwave passive filter design techniques, and phased-array antennas.

Dr. Simeoni is an Associate Member of the European Microwave Association.



Cristian I. Coman (S'04–M'06) was born in Timăveni, Romania, on March 14, 1972. He received the Engineer's degree from the Military Technical Academy, Bucharest, in 1996, and is currently working toward the Ph.D. degree in electrical engineering at the Delft University of Technology, Delft, The Netherlands.

His current interests include sparse array antennas, shared aperture antennas, computational electromagnetics, and radar signal processing.



Ioan E. Lager (M'01) was born in Braşov, Romania, on September 26, 1962. He received the Engineer's degree from Transilvania University, Braşov, Transilvania, in 1987, Ph.D. degree from the Delft University of Technology, Delft, The Netherlands, in 1996, and the Ph.D. degree from Transilvania University in 1998.

Since 1997, he has been with the Delft University of Technology, first with the Laboratory of Electromagnetic Research and, starting from 1998, with the International Research Centre for Telecommuni-

cations-Transmission and Radar, where he coordinates the applied electromagnetics related activities. He has authored one monograph and over 25 refereed publications. His principal scientific interests concern the (technological) design of antennas and the field of computational electromagnetics.